THE JOURNAL OF PHYSICAL CHEMISTRY C

Article

pubs.acs.org/JPCC

Chemical Stability toward O_2 and H_2O of Si(111) Grafted with $—CH_3$, $—CH_2CH_2CH_3$, $—CHCHCH_3$, and $—CCCH_3$

Federico A. Soria,[†] Patricia Paredes-Olivera,[‡] and Eduardo M. Patrito*[,†]

[†]Instituto de Investigaciones en Físico Química de Córdoba (INFIQC), CONICET-UNC, Departamento de Fisicoquímica and [‡]Departamento de Matemática y Física, Facultad de Ciencias Químicas, Universidad Nacional de Córdoba, Ciudad Universitaria, X5000HUA Córdoba, Argentina

Supporting Information

ABSTRACT: The chemical stability of compact monolayers on silicon toward oxidizing agents is a key issue for the use of such monolayers in devices such as solar cells or in the electronics industry. In this work, we investigated the reactivity toward H_2O, O_2, and OH species of monolayers terminated with a methyl group to unveil the mechanisms that prevent the oxidation of the underlying silicon. Density functional theory calculations were performed to investigate the reaction pathways for the two competing processes involved: diffusion through the monolayer and reaction with the terminal methyl group. Activation energy barriers for the diffusion of H_2O and O_2 are very sensitive to the monolayer structure, and they increase in the order $—CH_2—CH_2—CH_3$ < $—C≡C—CH_3$ < $—CH=CH—CH_3$ with energy barriers of 0.0 kcal/mol (0.0 kcal/mol), 35.0 kcal/mol (42.5 kcal/mol), and 57.0 kcal/mol (64.1 kcal/mol), respectively, for H_2O (O_2). This agrees with ordering of stabilities reported experimentally for these monolayers. The oxidation of the terminal methyl group by O_2 is less affected by steric constraints. The formation of the $—CH_2OOH$ species has an energy barrier of 56.5 kcal/mol on the rigid $—CH_3$ monolayer, whereas this barrier decreases to 40.7 kcal/mol on the $—C≡C—CH_3$ monolayer. In the case of the methyl monolayer, the abstraction of a H atom of the $—CH_3$ group has smaller energy barriers with singlet O_2 and OH reactants, with values of 38.4 and 3.5 kcal/mol, respectively. The high energy barriers of all of the processes investigated indicate that compact monolayers hinder the oxidation of the underlying substrate. The passivating capability of the monolayers correlates with the steric constraints for H_2O and O_2 diffusion.

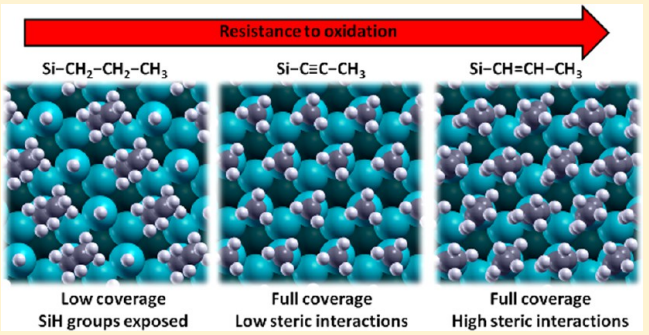

INTRODUCTION

The success of silicon in the electronics industry is based to a large extent on the properties of the silicon/oxide interface due to the excellent stability and passivating properties of SiO_2. For many applications such as molecular electronics on silicon, biochips, and solar cells, the oxide layer must be avoided to develop a well-defined linkage of organic molecules through silicon−carbon bonds.[1−3] In this context, the chemical stability toward oxidizing agents of compact monolayers on silicon can affect the performance of many devices.

Monoalayers based on *n*-alkanes are usually obtained by the reaction of 1-alkenes with the hydrogenated surface. Because of steric hindrance among the alkane chains, a maximum theoretical coverage of approximately 69% is predicted, implying that hydrogenated silicon atoms still remain on the surface.[4] This allows the penetration of oxygen molecules and the subsequent oxidation of silicon atoms. The oxidation of alkylated silicon(111) surfaces under ambient conditions produces inhomogeneous oxide patches on the surface composed of Si^+ and Si^{3+} species.[5] As the chain length increases, the oxidation of silicon atoms is inhibited. The X-ray photoelectron spectrum of the O 1s region of a $Si—C_{16}$ monolayer showed a lower O content than that of a $Si—C_{12}$ monolayer.[6]

In the case of alkanes, complete coverage of Si atop sites has been achieved only for the $—CH_3$ termination of Si(111), through the two-step chlorination/alkylation process.[7−9] However, after prolonged exposure to the environment, the oxidation of silicon atoms occurs.[5]

Therefore, the complete functionalization of all Si surface atoms with longer carbon chains is desirable to prevent silicon oxidation. This has been achieved by reaction of the hydrogenated surface with 1-alkynes.[10] Such densely packed monolayers are less prone to oxidation than is feasible by reaction of hydrogenated silicon with 1-alkenes.[11,12]

In a study of Si(111) surfaces functionalized with organic molecules having backbones of three carbon atoms[13,14] but with different C—C bonds close to the surface, it was found that the $Si—CH=CH—CH_3$ termination is more robust against surface oxidation and more stable against water attacks than Si—C≡

Received: August 29, 2014
Revised: November 27, 2014

DOI: 10.1021/jp508728v
J. Phys. Chem. C XXXX, XXX, XXX−XXX

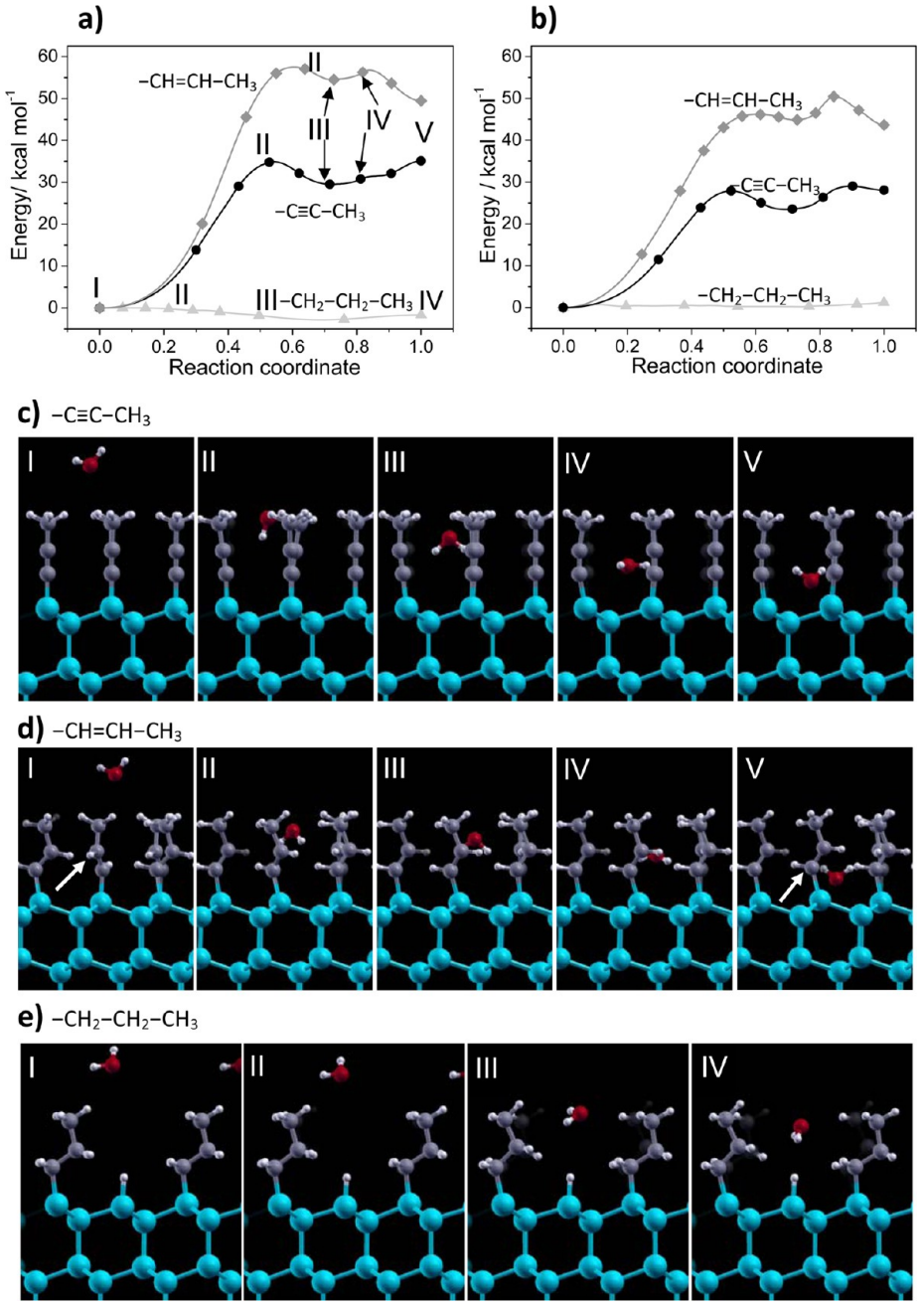

Figure 1. Energy profiles and structures for the diffusion of H_2O through the different monolayers. (a,b) Energy profiles obtained by (a) vdW-DFT and (b) standard DFT calculations. (c–e) Structures of the most representative points in the energy profiles for (c) —C≡C—CH_3, (d) —CH═CH—CH_3, and (e) —CH_2—CH_2—CH_3 monolayers. Calculations were performed using a 2 × 2 unit cell.

C—CH_3 and Si—CH_3, with all of these monolayers having full Si—C atop site terminations. The high stability of the Si—CH═CH—CH_3 layer was attributed to π–π interactions between the adjacent molecules, and it was also reported in the case of silicon nanowires.[15]

In a previous work, we used density functional theory (DFT) to investigate the reactivity of the hydrogenated Si(111) surface toward H_2O and O_2 to elucidate the mechanism of oxidation of the first silicon bilayer in air.[16] The perfect surface is unreactive toward H_2O and O_2 at room temperature, as deduced from the high energy barriers found. However, isolated Si dangling bonds surrounded by SiH groups readily react with O_2, initiating a radical propagation mechanism in which the oxidized Si radicals abstract H atoms from the neighboring SiH groups. This finally yields surface SiH groups with three Si—Si backbonds oxidized.[16] The protective character of an organic monolayer toward oxidation for the methyl termination has been investigated only theoretically.[17]

In the present work, we performed a DFT investigation of the reactivity of fully covered Si(111) surfaces in which every Si top atom is terminated with one of these functionalities: —CH_3, —CH═CH—CH_3, and —C≡C—CH_3. All of these monolayers have a terminal —CH_3 functionalilty, but they differ in the chain length and/or the hybridization of the inner carbon atoms. We considered the two possible pathways of (a) diffusion through the monolayer and reaction with the underlying silicon and (b) oxidation of the terminal methyl group. The stability of the monolayers was tested against the following reactants: H_2O,

DOI: 10.1021/jp508728v
J. Phys. Chem. C XXXX, XXX, XXX–XXX

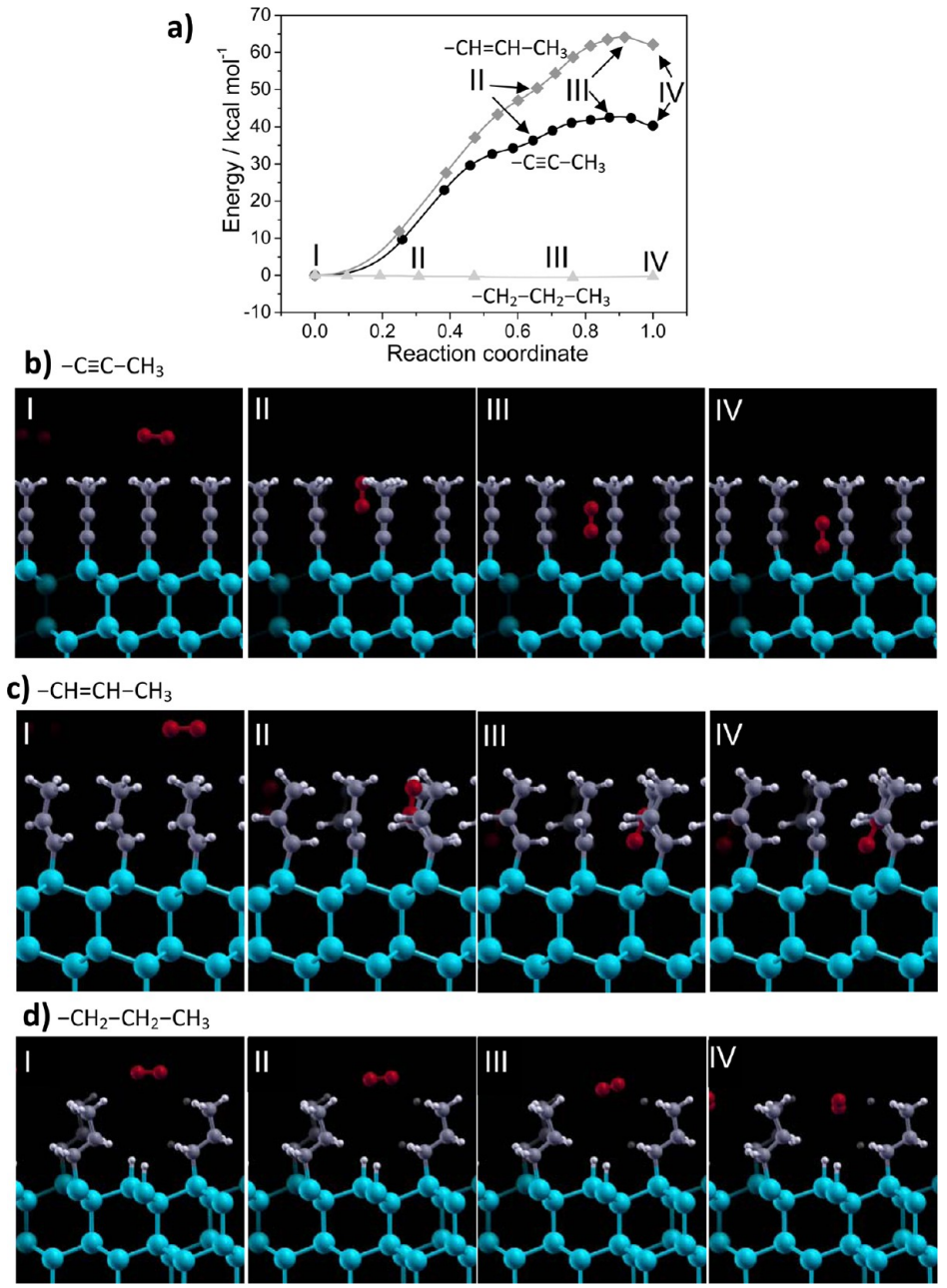

Figure 2. (a) Potential energy profiles along the reaction path for the diffusion of O_2 through the different monoalayers. (b–d) Structures of the most representative points in the energy profiles for (b) —C≡C—CH_3, (c) —CH═CH—CH_3, and (d) —CH_2—CH_2—CH_3 monolayers. Calculations were performed using a 2 × 2 unit cell.

triplet O_2, singlet O_2, and OH radical. We found that the oxidation of the underlying silicon requires the previous degradation of the monolayer. High energy barriers were found for the compact monolayers, and steric interactions were found to play a predominant role in the passivating capability of compact monolayers.

THEORETICAL METHODS AND SURFACE MODELING

Density functional theory (DFT) calculations were performed with the Quantum Espresso code,[18] in which the one-electron wave functions are expanded in a plane-wave basis set and the core electrons are described by norm-conserving ultrasoft pseudopotentials.[19] The Perdew–Burke–Ernzerhof (PBE) exchange and correlation functionals were employed.[20] The plane-wave expansion was done up to a kinetic-energy cutoff of 30 Ry (180 Ry for the density). The integration in the first Brillouin zone was performed with a (4 × 4 × 1) Monkhorst–Pack mesh.[21] All calculations involving O_2 were performed with spin polarization to adequately describe the triplet state of O_2. The diffusion of water through the monolayers was also investigated using a van der Waals functional (vdW-DFT).[22]

A silicon slab with six layers was used to model the (111) face of silicon. The slabs were separated by a vacuum thickness of 10 Å. The dangling bonds of the bottom surface were saturated with hydrogen atoms. We used a_0 = 5.48 Å for the lattice constant, as determined in a previous work.[23] The positions of all of the adsorbate atoms as well as those of the four topmost Si layers were fully optimized. The silicon atoms of the lower bilayer were

DOI: 10.1021/jp508728v
J. Phys. Chem. C XXXX, XXX, XXX–XXX

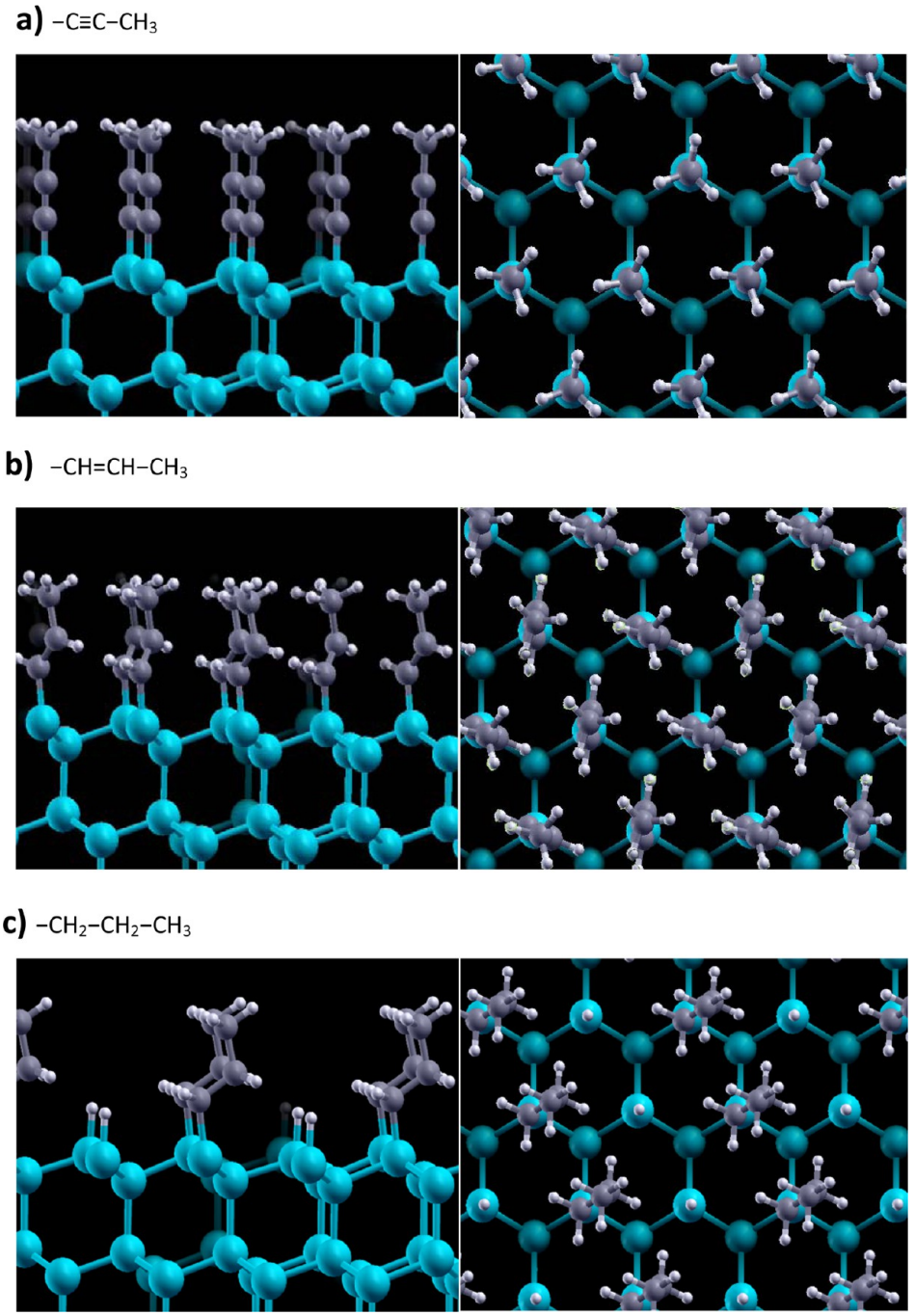

Figure 3. Side and top views of the equilibrium structures of (a) —C≡C—CH_3, (b) —CH═CH—CH_3, and (c) —CH_2—CH_2—CH_3 monolayers. The top views of the compact monolayers in panels a and b show that there is no free space for the diffusion of H_2O or O_2. On the contrary, the —CH_2—CH_2—CH_3 monolayer in panel c leaves the surface SiH groups exposed. Calculations were performed using a 2 × 2 unit cell.

kept fixed in a bulk configuration. Calculations were performed using 2 × 2 and 3 × 3 unit cells.

Reaction pathways and energy barriers were calculated with the climbing-image nudged-elastic-band (CI-NEB) method as implemented in the Quantum Espresso code.[24] After the CI-NEB calculation, we performed geometry optimizations using the geometries of the images on either side of the transition state (TS). When a TS effectively connects the initial and final points of the CI-NEB calculation, the geometry optimizations converge to these points. When this is not the case, the CI-NEB calculation is performed again with the initial and final states revisited, and the check is performed again.

RESULTS AND DISCUSSION

Diffusion of H_2O through —C≡C—CH_3, —CH═CH—CH_3, and —CH_2—CH_2—CH_3 Monolayers. Figure 1a shows the energy profiles along the reaction coordinate for the diffusion of a water molecule considering van der Waals interactions, whereas Figure 1b shows the energy profiles obtained with standard DFT. The corresponding structures of the vdW-DFT calculation are shown in Figure 1c−e for the —C≡C—CH_3, —CH═CH—CH_3, and —CH_2—CH_2—CH_3 monolayers, as indicated. Panel I shows the equilibrium structure of the adsorbed water molecule on the corresponding monolayer.

DOI: 10.1021/jp508728v
J. Phys. Chem. C XXXX, XXX, XXX−XXX

The highest energy barrier was obtained for —CH═CH—CH_3, with E_a = 57.0 kcal/mol, whereas the diffusional barrier for the —C≡C—CH_3 monolayer was found to be E_a = 35.0 kcal/mol. For the —CH_2—CH_2—CH_3 termination (with 50% surface coverage), the water molecule was found to penetrate the monolayer and absorb on top of a SiH group (panel IV in Figure 1e) in a process that is slightly exothermic (ΔE= −2.7 kcal/mol) and has no energy barrier. A weak hydrogen-bond interaction was found between the negatively charged hydrogen of the SiH surface group and the positively charged hydrogen atoms of the water molecule.

Panel II in Figure 1c,d corresponds to the structure of the transition state. It shows that the water molecule and the terminal methyl groups are located at approximately the same height above the plane of the silicon atoms. The panels in Figure 1c,d also show the deformation of the chains as the water molecule penetrates into the monolayer as a consequence of the strong repulsive interactions, which are evidenced by the ΔE values of 35.1 and 49.4 kcal/mol for the —C≡C—CH_3 (Figure 1c) and —CH═CH—CH_3 (Figure 1d) terminations, respectively. The higher ΔE and E_a values for the latter chain indicate that the hydrogen atoms of the sp^2 carbon atoms hinder the diffusion of H_2O through the monolayer. The arrow in panel V of Figure 1d shows that one alkene chain has to rotate to accommodate the water molecule.

Figure 1b shows the energy profiles calculated with standard DFT. The profiles are qualitatively similar to those obtained with vdW-DFT, but the energy barriers are approximately 6 kcal/mol lower for the —C≡C—CH_3 and —CH═CH—CH_3 monolayers. In the case of the —CH_2—CH_2—CH_3 layer, the standard DFT calculation shows virtually no interaction with the water molecule, whereas the vdW-DFT calculation gives an interaction of −2.7 kcal/mol.

Diffusion of O_2 through —C≡C—CH_3, —CH═CH—CH_3, and —CH_2—CH_2—CH_3 Monolayers. Figure 2a shows the energy profiles and Figure 2b−d shows the corresponding structures at different stages along the reaction path for O_2 diffusion through the monolayers. The energy barriers follow the same trend as in the case of the water molecule. The alkene monolayer has a higher barrier than the alkyne monolayer, with values of E_a = 64.1 and 42.5 kcal/mol, respectively, whereas there is no barrier for the alkane monolayer (with a 50% coverage). These calculations were performed with standard DFT, as the vdW functional has not yet been implemented in systems with spin polarization (the triplet state of O_2 in this case). These energy barriers are higher than for the water molecule, as expected from the larger size of the O_2 molecule. As shown in the last panel in Figure 2b,c, the diffusion of O_2 through the full-coverage monolayers produces a significant bending of the carbon chains. The shape of the energy profiles in Figure 2a shows that an O_2 molecule trapped within the monolayer will easily leave the monolayer with very low energy barriers (1.9 and 2.2 kcal/mol for the —C≡C—CH_3 and —CH═CH—CH_3 monolayers, respectively), unless it reacts with the silicon backbonds.

The diffusional barriers for H_2O and O_2 follow the same trend on the three monolayers: alkane < alkyne < alkene. The top views of the equilibrium structures of these monolayers shown in Figure 3 help to explain this trend. In the case of the linear —C≡C—CH_3 molecules (Figure 3a), which are perpendicular to the surface, there are channels among the molecules that allow diffusion. However, in the case of the alkene monolayer (Figure 3b), adjacent molecules are rotated in a configuration in which the hydrogen atoms of the chain hinder the penetration of molecules through the monolayer. The top view of the alkane monolayer (Figure 3c) shows that the surface SiH groups are readily accessible because of the lower coverage.

Silicon Oxidation by H_2O and O_2. We next investigated the reaction of H_2O and O_2 within the alkene and alkyne monoalyers with the silicon surface atoms. The reaction of H_2O breaks the Si—C bond, giving rise to a Si—OH surface species according to

$$\text{Si—CHCHCH}_3 + \text{H}_2\text{O} \rightarrow \text{Si—OH} + \text{CH}_2\text{CHCH}_3 \quad (1)$$

$$\text{Si—CCCH}_3 + \text{H}_2\text{O} \rightarrow \text{Si—OH} + \text{CHCCH}_3 \quad (2)$$

Figure 4a shows the corresponding energy profiles along the reaction path. The energy barriers are 27.4 and 28.3 kcal/mol for the —CH═CH—CH_3 and —C≡C—CH_3 monolayers, respectively. The reactions are very exothermic, with ΔE values of −75.6 and −49.8 kcal/mol, respectively. Panels II and II′ in Figure 4b show that, in the transition state, the Si—C bond is completely broken and the water molecule is adsorbed on the silicon radical. Panels III and III′ show that, in the final state, the alkene and alkyne molecules desorb from the monolayer. In a previous work,[23] we investigated the reactivity of Si—CH_2CH_3, Si—$CHCH_2$, and Si—CCH groups (surrounded by SiH groups) toward H_2O under low-coverage conditions. We observed that the presence of conjugation in the organic molecule lowers the energy barriers. We obtained values of 40.4, 33.7, and 29.2 kcal/mol, respectively. From a comparison of the structures of the transition states under full- and low-coverage conditions, we observed that the coverage has a significant effect on the

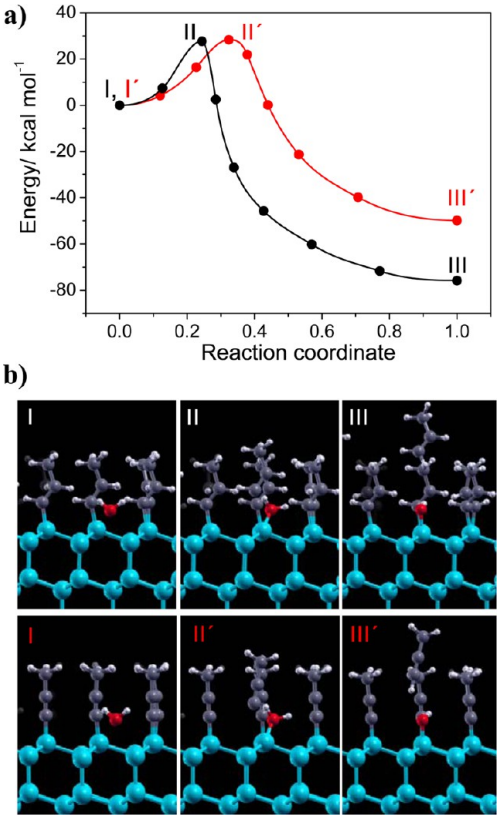

Figure 4. (a) Energy profiles for the reactions of H_2O with —CH═CH—CH_3 (black) and —C≡C—CH_3 (red) monolayers yielding a SiOH group and the desorbed molecule. (b) Critical points along the reaction paths. Calculations were performed using a 2 × 2 unit cell.

DOI: 10.1021/jp508728v
J. Phys. Chem. C XXXX, XXX, XXX−XXX

transition-state structures. Whereas, at low coverage, the organic molecules can tilt and the formation and breaking of bonds can occur in a concerted manner, at full coverage, the breaking of the Si—C bond occurs first because of the lower number of degrees of freedom.

The oxidation of the silicon backbonds by O_2 occurs in a reaction with two elementary steps. Figure 5a shows the energy profile and the corresponding structures for the first elementary step for the —C≡C—CH_3 monolayer. The double bond of O_2 is broken, and an intermediate is formed in which each oxygen atom is bound to a silicon atom (panel III in Figure 5b). The process occurs with an energy barrier of 17.7 kcal/mol. In the next step, two different reactions can occur: the oxidation of two Si—Si backbonds or the oxidation of one Si—Si backbond and one Si—C bond. The energy profiles of these processes are shown in Figure 5c, and the most representative structures are shown in Figure 5d. They have very low energy barriers (3.80 and 3.78 kcal/mol, respectively) and are very exothermic, with ΔE values of −149.0 and −129.6 kcal/mol, respectively. The ΔE values show that the oxidation of both silicon backbonds is more exothermic than the oxidation of one Si—Si backbond and one Si—C bond.

In the case of the —CH═CH—CH_3 monolayer, similar energy barriers were obtained. The corresponding structures and energy profiles are shown in Figure S1 of the Supporting Information. The formation of the oxygen intermediate occurs with an energy barrier of 19.2 kcal/mol, and next, the oxidation of two Si—Si backbonds or the oxidation one Si—Si backbond and one Si—C occurs with a very small barrier of 0.46 kcal/mol (Figure S2, Supporting Information).

In summary, the rate-determining step for the oxidation of the silicon backbonds by O_2 is the formation of an O—O intermediate bound to three silicon atoms (panel III in Figure 5b), with energy barriers of 17.7 and 19.2 kcal/mol for the —C≡C—CH_3 and —CH═CH—CH_3 monolayers, respectively. These values are to be compared with the energy barriers for silicon oxidation by water: 28.3 and 27.4 kcal/mol, respectively. The barriers are roughly 10 kcal/mol higher when water is the oxidizing agent than when oxygen is the oxidizing agent, indicating that the latter is a better oxidant.

In a previous work,[16] we investigated the different mechanisms of oxidation of hydrogenated Si(111) by O_2. For the oxidation of Si—Si backbonds of adjacent Si atoms, we obtained a barrier of 22.8 kcal/mol in a reaction with ΔE = −117.9 kcal/mol.[16] The lower energy barriers and more negative ΔE values of the grafted surfaces are a consequence of the destabilizing effect of the strain of the O_2 molecule within the monolayers, which thus makes it more reactive. The O_2 molecule within the —CH═CH—CH_3 monolayer has a bond length of 1.321 Å, whereas O_2 adsorbed on top of the monolayer has a bond length of 1.242 Å. Therefore, the lengthening of the bond makes the more reactive.

Figure 6 summarizes the overall energy profiles for the diffusion and silicon oxidation processes for O_2 and H_2O. The oxidation of the silicon backbonds by O_2 has a global energy barrier of 82.9 kcal/mol for the Si—CH═CH—CH_3 monolayer and 58.1 kcal/mol for the Si—C≡C—CH_3 monolayer, whereas the ΔE values are −96.1 and −108.2 kcal/mol, respectively. In the case of H_2O, the formation of SiOH surface groups has energy barriers of 77.1 and 63.4 kcal/mol for the Si—CH═CH—CH_3 and Si—C≡C—CH_3 monolayers, respectively. For both oxidants, the alkene monolayer has the highest energy barriers.

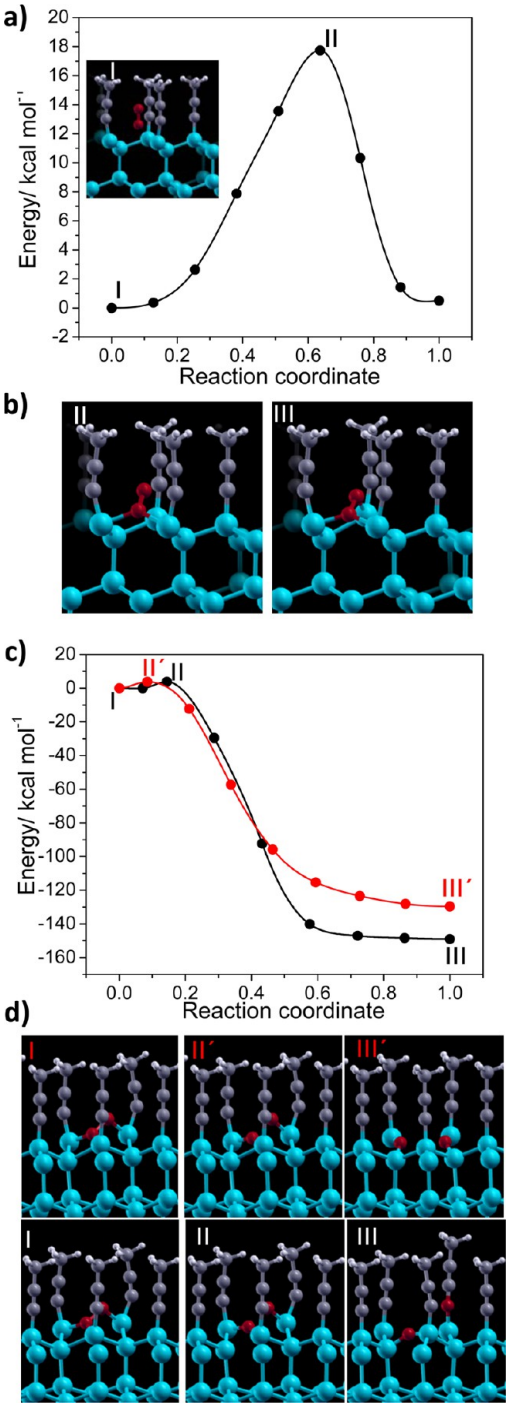

Figure 5. Reaction of O_2 within a —C≡C—CH_3 monolayer with the underlying silicon substrate: (a) Energy profile along the reaction path for the formation of an O_2 intermediate tricoordinated to silicon atoms. (b) Structures of the transition state (panel II) and O_2 intermediate (panel III). (c) Energy profiles for the insertion of O atoms into two Si—Si backbonds (red) and into Si—Si and Si—C bonds (black). (d) Structures of representative points in the energy profiles. Calculations were performed using a 2 × 2 unit cell.

We can now address the factors that influence the different reactivities of the monolayers. The oxidation of silicon grafted with a —CH_2—CH_2—CH_3 monolayer occurs after 1 day of exposure to air.[5,14] In the case of —C≡C—CH_3, the oxidation begins after 25 days of exposure to air, whereas for the —CH═

DOI: 10.1021/jp508728v
J. Phys. Chem. C XXXX, XXX, XXX−XXX

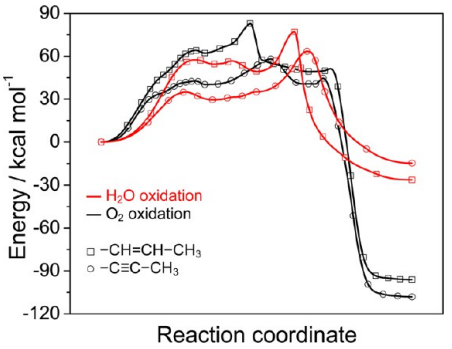

Figure 6. Total energy profiles for the diffusion and silicon oxidation processes for O_2 and H_2O oxidants on (□) —CH═CH—CH_3 and (○) —C≡C—CH_3 monolayers.

CH—CH_3 monolayer, the oxidation occurs after 65 days of exposure to air.[13,14]

The fact that silicon grafted with the —CH_2—CH_2—CH_3 monolayer readily oxidizes is expected, as full coverage cannot be obtained with alkane monolayers. As shown in Figures 1a and 2a, the diffusion of H_2O and O_2 through the monolayer occurs with no energy barrier in the case of 50% surface coverage. Thus, the molecules can reach the SiH groups and oxidize silicon with much lower energy barriers, as we discussed in previous works.[16,23] However, if a full-coverage alkane monolayer coud be obtained, its blocking properties would still be better than those of the other monolayers. We calculated the ΔE value for the insertion of O_2 into a full-coverage propane monolayer (the equilibrium structure is shown in Figure S3, Supporting Information) and obtained a value of 66.8 kcal/mol, which is larger than the ΔE values of 62.2 and 40.3 kcal/mol for the alkene and alkyne monolayers, respectively (Figure 2).

Haick and co-workers[14] proposed that the trend observed for the —CH═CH—CH_3 and —CH═CH—CH_3 monolayers arises from the nature of the C—C bond nearest the silicon surface. They attributed the higher reactivity of the alkyne monolayer to a partial transfer of one π-electron pair of the triple bond to the Si atop atom, thus enhancing the reactivity of this Si atom toward oxidizing agents. We observed this trend; however, the differences are small. As discussed above, the reaction of O_2 inserted within the monolayer with the silicon backbonds has an energy barrier of 17.7 kcal/mol for the —C≡C—CH_3 monolayer (Figure 4) and 19.2 kcal/mol for the —CH═CH—CH_3 monolayer (see Figure S1, Supporting Information). Therefore, the Si atoms of the former monolayer are slightly more reactive, as anticipated by Haick and co-workers.[14] However, our results indicate that the differences in reactivity toward oxidation mainly arise from steric effects during the diffusion of O_2 through the monolayer. Thus, the best passivating —CH═CH—CH_3 monolayer has the highest diffusional barrier (64.1 kcal/mol), whereas the —C≡C—CH_3 monolayer has a lower barrier (42.5 kcal/mol), and the —CH_2—CH_2—CH_3 monolayer has no barrier. The same trend is observed for the water molecule, with diffusional energy barriers of 57.0, 35.0, and 0.0 kcal/mol, respectively. For each monolayer, the diffusional barriers for H_2O are smaller than those for O_2, as expected from the smaller molecular size of H_2O, once again indicating that steric factors predominate. The global energy barriers for the diffusion and silicon oxidation process (Figure 6) show that the differences in reactivities between the alkene- and alkyne-grafted silicon surfaces are more pronounced for O_2 than for H_2O, as steric constraints are more important for O_2.

It is also important to consider whether imperfections in the alkene and alkyne monolayers could be responsible for the differences in reactivities. If this were the case, we would expect no major differences between the two monolayers, as the appearance of defects is random. However, the stability of silicon grafted with these monolayers shows pronounced differences when exposed to air. The oxidation of alkyne-grafted silicon occurs after 25 days, whereas that of alkene-grafted silicon begins after 65 days. The alkyne monolayer is the most studied in the literature, and different reports claim that it can be obtained with 100% surface coverage.[13,14,25] However, this monolayer has a lower resistance to oxidation than the alkene monolayer. This implies that the differences in the passivating properties can be ascribed to the nature of the carbon chains and not to imperfections.

Methyl Group and Si—Si Backbond Oxidation of the Si—CH_3 Monolayer. Figure 7a shows the energy profile in the reaction of O_2 with the Si—CH_3 monolayer. The most representative structures along the energy profile are shown in Figure 7b. Molecular oxygen cannot penetrate intact into the methylated surface to reach the silicon backbonds. The panels in Figure 7b show that, as O_2 approaches the methyl group, it

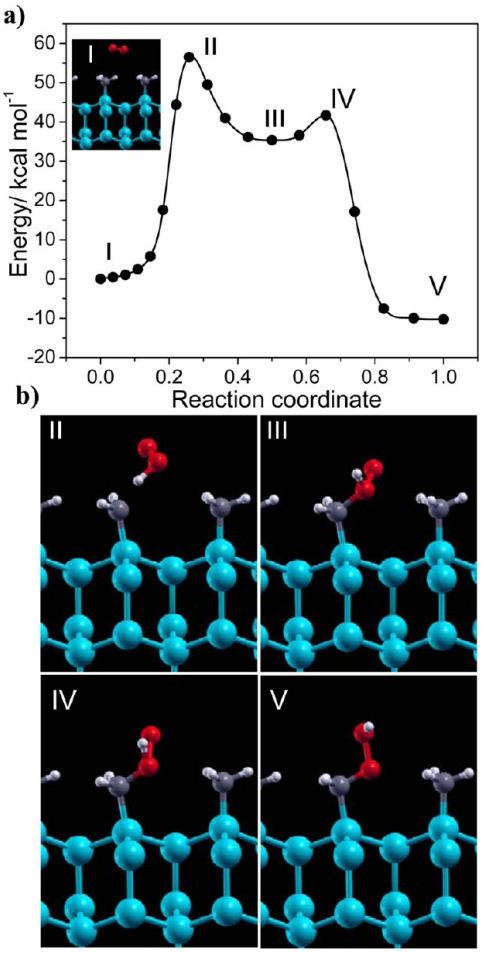

Figure 7. (a) Energy profile along the reaction path for hydrogen abstraction from a methyl group by O_2 to yield the $SiCH_2OOH$ product. The inset corresponds to the reactants. (b) Structures of the most representative points along the energy profile. Panels II and IV correspond to TS structures, whereas panel III corresponds to the structure of the intermediate. The $SiCH_2OOH$ product is shown in panel V.

DOI: 10.1021/jp508728v
J. Phys. Chem. C XXXX, XXX, XXX−XXX

abstracts a H atom, and the OOH radical thus formed (panel II) binds to the C atom (panel III) to finally yield the Si—CH_2OOH product (panel V). In this respect, the methylated surface is different from the —C≡C—CH_3- and —CH═CH—CH_3-terminated surfaces, which allow the diffusion of O_2 through the monolayer. This is a consequence of the lack of degrees of freedom of the rigid methylated surface, whereas the distortion of the carbon chains in the alkyne and alkene monolayers allows the penetration of the O_2 molecule.

Figure 7a shows that the formation of the Si—CH_2OOH moiety (panel V) occurs in two steps. The first step has a barrier of 56.5 kcal/mol and corresponds to the transfer of a H from the methyl group to O_2, yielding the Si—CH_2—OH—O intermediate (panel III). Finally, the H atom is transferred to the terminal O atom with a barrier of 6.3 kcal/mol (TS in panel IV), yielding the Si—CH_2OOH product. The overall reaction is exothermic with $\Delta E = -10.2$ kcal/mol.

The abstraction of a H atom from —CH_3 has a much higher energy barrier than the direct insertion of O atoms into the Si backbonds (22.8 kcal/mol) of the hydrogenated surface.[16] This implies that any defect in the methylation process leaving unreacted SiH groups will readily induce oxidation at monolayer defects.

The next elementary steps originate from the breaking of the O—O bond of the —COOH group and the reaction of the released OH radical with the surrounding H atoms to yield H_2O and other species. We found the following elementary reaction steps for dehydrogenation reactions

$$\text{Si—CH}_2\text{OOH} \rightarrow \text{Si—CHO} + \text{H}_2\text{O} \quad (3)$$

$$\text{Si—CH}_2\text{OOH} + \text{Si—CH}_3 \rightarrow \text{Si}^{\bullet} + \text{H}_2\text{CO} + \text{Si═CH}_2 + \text{H}_2\text{O} \quad (4)$$

Figure 8a shows the energy profile for reaction 3, in which the OH radical abstracts a H atom from the Si—CH_2OOH group. The corresponding structures are shown in Figure 8b. The energy profile of reaction 4, in which the OH radical abstracts a H atom from a neighboring methyl group, is shown in Figure 8c, and the most representative structures along the reaction path are shown in Figure 8d. The energy profiles in Figure 8a,c show that the two reactions have similar energy barriers (25.1/mol and 22.1 kcal/mol, respectively), as the transition states correspond to the breakage of the O—O bond of the —COOH group (panel III in Figure 8b,d).

Figure 8b shows that the reaction products are H_2O and a Si—CHO surface group (panel V), whereas in Figure 8d, the products are formaldehyde, water, and a surface Si═CH_2 group (panel V). The desorption of formaldehyde occurs with a barrier of 8.5 kcal/mol and leaves a surface silyl radical.

Reaction 3 is very exothermic with $\Delta E = -54.1$ kcal/mol (Figure 8a), whereas reaction 2 is slightly endothermic with $\Delta E =$ 1.2 kcal/mol, as an unstable surface silyl radical is formed (Figure 8c).

Further reactions of OH radicals with dehydrogenated surface groups give rise to alcohols and carboxyl groups. Because of the high reactivity of OH, we anticipate low energy barriers, although this isue is beyond the scope of this work. Reaction 4 opens a path for the oxidation of the silicon substrate, as it leaves a surface silyl radical, which readily reacts with O_2, as we discussed in a previous work.[16]

An O atom from the Si—CH_2—OOH species can also be transferred to a silicon backbond. The reaction occurs in two

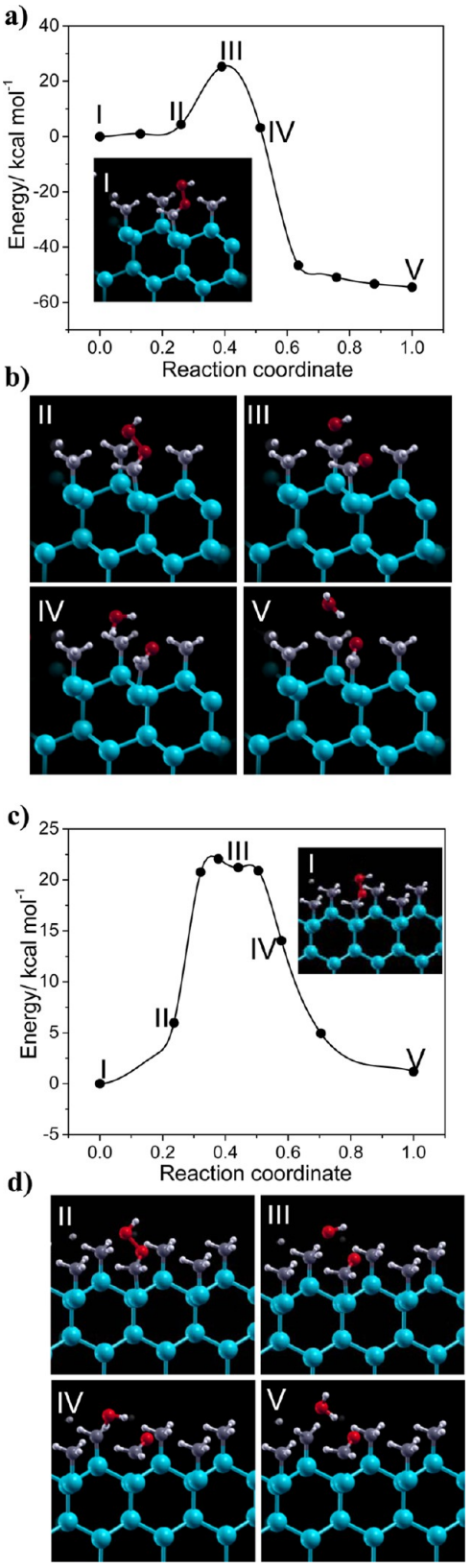

Figure 8. (a) Energy profile for breakage of the $SiCH_2O$—OH bond (panel I) together with hydrogen abstraction by OH to yield the SiCHO + H_2O products (panel V). (b) Representative structures along the reaction path. (c) Energy profile for breakage of the $SiCH_2O$—OH bond together with hydrogen abstraction from an adjacent methyl group to yield a silyl radical, H_2CO, and H_2O. Calculations performed using a 3 × 3 unit cell. (d) Representative structures along the reaction path.

DOI: 10.1021/jp508728v
J. Phys. Chem. C XXXX, XXX, XXX−XXX

elementary steps. In the first step, the O atom is inserted into the Si—C bond

$$Si—CH_2—OOH \rightarrow - Si—O—CH_2—OH \quad (5)$$

and in the next step, the O atom is transferred to the Si—Si backbond

$$Si—Si—O—CH_2—OH \rightarrow Si—O—Si—CH_2—OH \quad (6)$$

The first elementary step has a barrier of 22.1 kcal/mol, whereas the second has a barrier of 72.9 kcal/mol (energy profiles in Figure S4, Supporting Information). Therefore, we conclude that the insertion of O atoms into silicon backbonds from oxidized methyl groups is unlikely on account of the high energy barriers. In the case of the methyl monolayer, silicon oxidation likely proceeds after reaction 4, which leaves a reactive silyl radical that can react with O_2, leading to the oxidation of the silicon backbonds.[16]

Oxidation of the Methyl Group of Si—C≡C—CH_3 and Si—CH═CH—CH_3 Monolayers. Figure 9a shows the energy profile for the reaction of the terminal methyl group of Si—C≡C—CH_3 with O_2. The reaction occurs in two steps with an intermediate of the form Si—C≡C—CH_2—OH—O in which one of the H atoms of the methyl group is transferred to the O atom bound to the C atom (panel III in Figure 9b). The energy barrier for the overall reaction is 40.7 kcal/mol, with $\Delta E = -9.2$ kcal/mol. This barrier is nearly 15 kcal/mol lower than the barrier to obtain the Si—CH_2—OOH moiety on the fully methylated surface (with E_a = 56.5 kcal/mol, Figure 7a). The tilting of the Si—C bond of Si—CH_2OOH with respect to the surface normal is higher than for Si—$CCCH_2$OOH (7.2° vs 1.0°, respectively). This indicates that the steric constraints of the rigid methylated surface are responsible for the higher energy barriers. An equivalent calculation in the case of the Si—CH═CH—CH_3 monolayer yields an energy barrier of 37.1 kcal/mol with an exothermicity of $\Delta E = -11.9$ kcal/mol (energy profiles and representative structures along the reaction path in Figure S5, Supporting Information). Therefore, the alkyne and alkene monolayers have similar barriers for the oxidation of the terminal methyl group to —CH_2OOH.

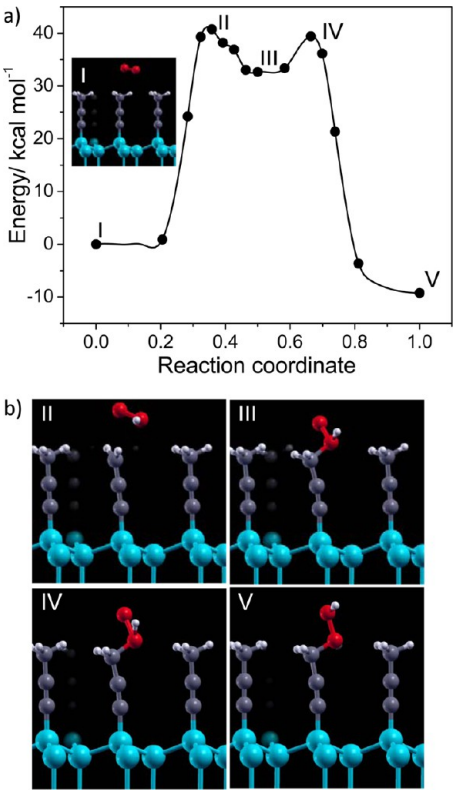

Figure 9. a) Energy profile for the reaction of O_2 with the terminal methyl group of the —C≡C—CH_3 monolayer to yield the —C≡C—CH_2OOH product. The inset shows the initial structure. (b) Most representative structures along the reaction path. The reaction has two steps with an intermediate shown in panel III. The panels show the distortion of the monolayer as the reaction proceeds.

The breakage of the O—O bond of the terminal —CH_2OOH group can give rise to polymerization reactions that are highly exothermic. The OH radical abstracts a H atom from the methyl group of an adjacent chain, and both chains become bonded by the remaining O atom according to

$$Si—R—CH_3 + Si—R—COOH \rightarrow Si—R—CH_2—O—CH_2—R—Si + H_2O \quad (7)$$

where R represents the rest of the carbon chain. We obtained very exothermic values with $\Delta E = -54.4$ and -47.1 kcal/mol for the alkyne and alkene monolayers, respectively. The corresponding equilibrium structures are shown in Figure S6 (Supporting Information).

The energetics of this section shows that the oxidation of the terminal methyl groups to produce either a —COOH moiety or intralayer bonds according to reaction 7 is not very sensitive to the nature of the underlying carbon chain (alkene vs alkyne). This is to be expected, as the oxidation of the methyl groups is a surface reaction in which the rest of the carbon chain is not involved except for some relaxation.

This is not the case for the oxidation of silicon atoms, which requires the diffusion of the oxidizing species (O_2 or H_2O) through the carbon chains. Therefore, we do not expect the oxidation of the terminal methyl groups to have a major influence on the oxidation of silicon atoms unless it interferes with the diffusion of species through the monolayer. The oxidation of the terminal methyl group to yield the bulky —CH_2OOH group might even add some additional steric restraints on the diffusion of O_2 or H_2O. Therefore, the partial oxidation of methyl groups might have a passivating effect. In a study of the controlled oxidation of alkyl monolayers on silicon using plasma treatment, it was found that the Si substrate remains oxygen-free after the oxidation of the top layer,[26] thus showing the passivating effect of the oxidized layer.

Beyond the energetic analysis of this section, we believe that the surface dynamics has to be considered to address the oxidation of the terminal methyl group. The methyl group rotates about the C—C bond, and this probably hinders impinging O_2 molecules from reacting, thus leading to the desorption of O_2. On the other hand, O_2 molecules reaching the surface at hollow sites among methyl groups (see top views in Figure 3a,b) can penetrate into the monolayer if they have enough kinetic energy to finally reach the silicon backbonds.

Reactions with Singlet O_2 and OH Radicals. Oxygen plasma treatments of low power density are employed to functionalize organic monolayers by introducing surface polar groups.[26,27] The dominant reactive species at low power density is the singlet oxygen molecule.[27] We therefore also considered the reaction of singlet O_2 with the Si—CH_3 and Si—C≡C—CH_3 monolayers to evaluate the impact of the electronic state of O_2 on the surface reactivity. The reaction on both monolayers

DOI: 10.1021/jp508728v
J. Phys. Chem. C XXXX, XXX, XXX−XXX

has two elementary steps, as in the case of the triplet state. However, there is an overall decrease in energy barriers.

The reaction with the methylated surface (Figure 10a) has an energy barrier of 38.7 kcal/mol which implies a reduction of nearly 18 kcal/mol as compared to the reaction with triplet oxygen (Figure 7a). The barrier to convert the intermediate (panel III in Figure 10b) into the final product is also very small: 6.2 kcal/mol.

For the Si—C≡C—CH_3 monolayer, the energy barrier is 24.3 kcal/mol (Figure 10c), which is nearly 16 kcal/mol lower than in the case of the reaction with triplet O_2 (Figure 9a), and the barrier for the conversion of the intermediate (panel III in Figure 10d) into the final product (panel V) is also very small: 6.8 kcal/mol.

As the O_2 molecule is in an excited state, the reactions are more exothermic than in the case of triplet O_2, with ΔE values of −28.1 kcal/mol (Si—CH_3) and −25.6 kcal/mol (Si—$CCCH_3$). The corresponding values for the reactions with triplet O_2 are −10.0 and −9.23 kcal/mol, respectively.

OH radicals react with the hydrogenated surface yielding silyl radicals in a reaction that occurs with virtually no energy barrier.[16] As discussed in previous sections, the fully methylated silicon surface provides superior passivation in the reaction with O_2. We now consider its protective character toward OH radicals. Under ambient conditions during day time, when solar cells are operative, OH radicals are present in the atmosphere, and the degradation of the surface can produce deleterious surface charge recombination processes. In this context, we consider the reactivity of the fully methylated silicon surface with OH radicals.

OH radicals can be involved in an hydrogen abstraction reaction or in the reaction with the C atom of the methyl group

$$SiCH_3 + OH \rightarrow SiCH_2 + H_2O \quad (8)$$

$$SiCH_3 + OH \rightarrow Si^{\bullet} + CH_3OH \quad (9)$$

The first reaction yields water, whereas the second produces methanol and a reactive surface silyl radical. The corresponding energy profiles along the reaction path are shown in Figure 11a for reaction 8 and in Figure 11b for reaction 9. Hydrogen abstraction reaction 8 has a small barrier of 3.5 kcal/mol, whereas reaction 9 has a barrier of 17.0 kcal/mol. The magnitudes of these barriers indicate that the methyl monolayer is not capable of protecting the surface against oxidation when exposed to atmospheric conditions for the prolonged times required in a solar cell. Therefore, an increase of the chain length of the alkyl molecules is required, but this has the disadvantage of reducing the surface coverage and leaving hydrogenated silicon atoms. However, a recent experimental work showed that this problem can be circumvented by using a mixed methyl/allyl monolayer, which produces efficient surface passivation for use in solar cells.[28]

CONCLUSIONS

In this work we investigated the chemical stability of alkane, alkene, and alkyne monolayers terminated with a methyl group considering H_2O, triplet O_2, singlet O_2, and OH oxidizing species to unveil the mechanisms involved in the oxidation of the monolayers and the oxidation of the underlying silicon substrate.

The oxidizing species can diffuse through the monolayers or react with the terminal methyl group. The energy barriers for the diffusion of O_2 and H_2O are very sensitive to the monolayer structure, indicating that steric interactions play a predominant role. The diffusional barriers for H_2O and O_2 follow the same trend on the three monolayers, namely, alkane < alkyne < alkene,

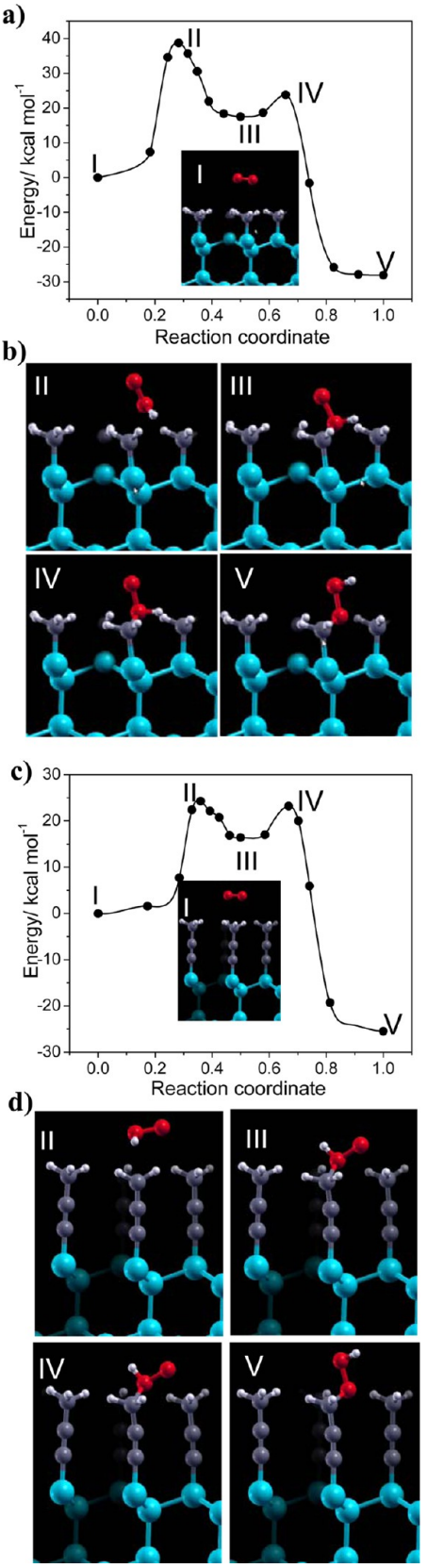

Figure 10. Reactions with the O_2 molecule in the singlet state: (a,c) energy profiles and (b,d) structures for the reactions with the (a,b) methylated and (c,d) —C≡C—CH_3-terminated surfaces.

DOI: 10.1021/jp508728v
J. Phys. Chem. C XXXX, XXX, XXX−XXX

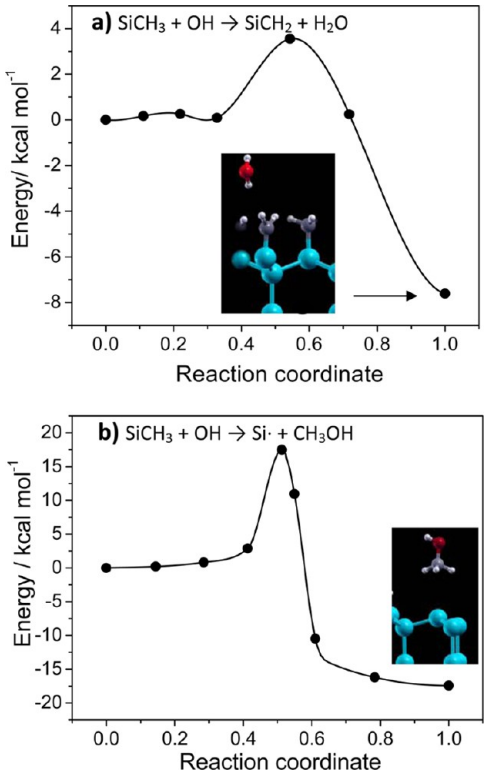

Figure 11. Energy profiles for the reaction of the methylated surface with OH radicals to yield (a) H_2O by a hydrogen abstraction reaction and (b) CH_3OH by insertion at the C atom. The insets show the equilibrium structures of the final products.

which coincides with the experimentally observed stability[15] upon exposure to air. Thus, the best passivating —CH═CH—CH_3 monolayer has the highest diffusional barrier for O_2 (64.1 kcal/mol), whereas diffusion through the —C≡C—CH_3 monolayer has a lower barrier (42.5 kcal/mol), and there is no barrier in the case of —CH_2—CH_2—CH_3 when its coverage is less than 100%.

Once the oxidizing molecule is within the monolayer, the oxidation of silicon is not very sensitive to the nature of the carbon chain, with O_2 being a better oxidant than H_2O. The oxidation of the silicon backbonds by O_2 occurs with energy barriers of 17.7 and 19.2 kcal/mol for the —C≡C—CH_3 and —CH═CH—CH_3 monolayers, respectively. In the case of water, the barriers for silicon oxidation to SiOH increase to 28.3 and 27.4 kcal/mol, respectively.

The oxidation of the terminal methyl group by O_2 is not very sensitive to the nature of the underlying carbon chain (alkene vs alkyne), as it is a surface reaction in which the chain is not primarily involved. Upon oxidation of —CH_3, the —CH_2OOH species is produced with activation barriers of 37.1 and 40.7 kcal/mol for the —CH═CH—CH_3 and —C≡C—CH_3 monolayers, respectively. In the case of the rigid Si—CH_3 monolayer, the barrier increases to 56.5 kcal/mol. The oxidation process continues as OH radicals are released from the breaking of the O—O bond of —CH_2OOH. They can react with the surrounding molecules in hydrogen abstraction or oxidation reactions. The —CH_2OOH-terminated alkene and alkyne monolayers can also undergo polymerization reactions by oxygen bonding between adjacent molecules. The oxidation of terminal methyl groups can have a passivating effect with respect to the silicon oxidation by introducing additional steric restraints on the diffusion of O_2 and H_2O. When singlet O_2 is the reactant, the activation energy decreases to 38.4 and 27.7 kcal/mol for the —CH_3 and —C≡C—CH_3 monolayers, respectively.

■ ASSOCIATED CONTENT

Ⓢ Supporting Information

Additional figures as described in the text. This material is available free of charge via the Internet at http://pubs.acs.org.

■ AUTHOR INFORMATION

Corresponding Author

*Phone: 54-351-4344972. E-mail: martin@fcq.unc.edu.ar.

Notes

The authors declare no competing financial interest.

■ ACKNOWLEDGMENTS

Financial support from CONICET (PIP 5903) and SECYT-UNC is gratefully acknowledged. F.A.S. thanks CONICET for a doctoral fellowship.

■ REFERENCES

(1) Li, Y.; Calder, S.; Yaffe, O.; Cahen, D.; Haick, H.; Kronik, L.; Zuilhof, H. Hybrids of Organic Molecules and Flat, Oxide-Free Silicon: High-Density Monolayers, Electronic Properties, and Functionalization. *Langmuir* **2012**, *28*, 9920−9929.

(2) Vilan, A.; Yaffe, O.; Biller, A.; Salomon, A.; Kahn, A.; Cahen, D. Molecules on Si: Electronics with Chemistry. *Adv. Mater.* **2010**, *22*, 140−159.

(3) Buriak, J. M. Illuminating Silicon Surface Hydrosilylation: An Unexpected Plurality of Mechanisms. *Chem. Mater.* **2014**, *26*, 763−772.

(4) Scheres, L.; Rijksen, B.; Giesbers, M.; Zuilhof, H. Molecular Modeling of Alkyl and Alkenyl Monolayers on Hydrogen-Terminated Si(111). *Langmuir* **2011**, *27*, 972−980.

(5) Webb, L. J.; Michalak, D. J.; Biteen, J. S.; Brunschwig, B. S.; Chan, A. S. Y.; Knapp, D. W.; Meyer, H. M.; Nemanick, E. J.; Traub, M. C.; Lewis, N. S. High-Resolution Soft X-ray Photoelectron Spectroscopic Studies and Scanning Auger Microscopy Studies of the Air Oxidation of Alkylated Silicon(111) Surfaces. *J. Phys. Chem. B* **2006**, *110*, 23450−23459.

(6) Lavi, A.; Cohen, H.; Bendikov, T.; Vilan, A.; Cahen, D. Si−C-bound Alkyl Chains on Oxide-Free Si: Towards Versatile Solution Preparation of Electronic Transport Quality Monolayers. *Phys. Chem. Chem. Phys.* **2011**, *13*, 1293−1296.

(7) Bansal, A.; Li, X.; Lauermann, I.; Lewis, N. S.; Yi, S. I.; Weinberg, W. H. Alkylation of Si Surfaces Using a Two-Step Halogenation/Grignard Route. *J. Am. Chem. Soc.* **1996**, *118*, 7225−7226.

(8) Yu, H.; Webb, L. J.; Ries, R. S.; Solares, S. D.; Goddard, W. A., III; Heath, J. R.; Lewis, N. S. Low-Temperature STM Images of Methyl-Terminated Si(111) Surfaces. *J. Phys. Chem. B* **2005**, *109*, 671−674.

(9) Nemanick, E. J.; Hurley, P. T.; Brunschwig, B. S.; Lewis, N. S. Chemical and Electrical Passivation of Silicon (111) Surfaces through Functionalization with Sterically Hindered Alkyl Groups. *J. Phys.Chem. B* **2006**, *110*, 14800−14808.

(10) Scheres, L.; Arafat, A.; Zuilhof, H. Self-Assembly of High-Quality Covalently Bound Organic Monolayers onto Silicon. *Langmuir* **2007**, *23*, 8343−8346.

(11) Scheres, L.; Giesbers, M.; Zuilhof, H. Self-Assembly of Organic Monolayers onto Hydrogen-Terminated Silicon: 1-Alkynes Are Better Than 1-Alkenes. *Langmuir* **2010**, *26*, 10924−10929.

(12) Scheres, L.; Giesbers, M.; Zuilhof, H. Organic Monolayers onto Oxide-Free Silicon with Improved Surface Coverage: Alkynes versus Alkenes. *Langmuir* **2010**, *26*, 4790−4795.

(13) Puniredd, S. R.; Assad, O.; Haick, H. Highly Stable Organic Modification of Si(111) Surfaces: Towards Reacting Si with Further Functionalities while Preserving the Desirable Chemical Properties of

DOI: 10.1021/jp508728v
J. Phys. Chem. C XXXX, XXX, XXX−XXX

Full Si−C Atop Site Terminations. *J. Am. Chem. Soc.* **2008**, *130*, 9184−9185.
(14) Puniredd, S. R.; Assad, O.; Haick, H. Highly Stable Organic Monolayers for Reacting Silicon with Further Functionalities: The Effect of the C−C Bond Nearest the Silicon Surface. *J. Am. Chem. Soc.* **2008**, *130*, 13727−13734.
(15) Bashouti, M. Y.; Sardashti, K.; Schmitt, S. W.; Pietsch, M.; Ristein, J.; Haick, H.; Christiansen, S. H. Oxide-Free Hybrid Silicon Nanowires: From Fundamentals to Applied Nanotechnology. *Prog. Surf. Sci.* **2013**, *88*, 39−60.
(16) Soria, F. A.; Patrito, E. M.; Paredes-Olivera, P. Oxidation of Hydrogenated Si(111) by a Radical Propagation Mechanism. *J. Phys. Chem. C* **2012**, *116*, 24607−24615.
(17) Li, H.; Lin, Z.; Wu, Z.; Luska, M. T. First Principles Analysis of the Initial Oxidation of Si(001) and Si(111) Surfaces Terminated with H and CH_3. *J. Chem. Phys.* **2012**, *136*, 064507.
(18) Giannozzi, P.; Baroni, S.; Bonini, N.; Calandra, M.; Car, R.; Cavazzoni, C.; Ceresoli, D.; Chiarotti, G. L.; Cococcioni, M.; Dabo, I.; Dal Corso, A.; de Gironcoli, S.; Fabris, S.; Fratesi, G.; Gebauer, R.; Gerstmann, U.; Gougoussis, C.; Kokalj, A.; Lazzeri, M.; Martin-Samos, L.; Marzari, N.; Mauri, F.; Mazzarello, R.; Paolini, S.; Pasquarello, A.; Paulatto, L.; Sbraccia, C.; Scandolo, S.; Sclauzero, G.; Seitsonen, A. P.; Smogunov, A.; Umari, P.; Wentzcovitch, R. M. QUANTUM ESPRESSO: A Modular and Open-Source Software Project for Quantum Simulations of Materials. *J. Phys.: Condens. Matter* **2009**, *21*, 395502−395521.
(19) Vanderbilt, D. Soft Self-Consistent Pseudopotentials in a Generalized Eigenvalue Formalism. *Phys. Rev. B* **1990**, *41*, 7892−7895.
(20) Perdew, J. P.; Burke, K.; Ernzerhof, M. Generalized Gradient Approximation Made Simple. *Phys. Rev. Lett.* **1996**, *77*, 3865−3868.
(21) Monkhorst, H. J.; Pack, J. D. Special Points for Brillouin-Zone Integrations. *Phys. Rev. B* **1976**, *13*, 5188−5192.
(22) Roman-Perez, G.; Soler, J. M. Efficient Implementation of a van der Waals Density Functional: Application to Double-Wall Carbon Nanotubes. *Phys. Rev. Lett.* **2009**, *103*, 096102.
(23) Juarez, M. F.; Soria, F. A.; Patrito, E. M.; Paredes-Olivera, P. Influence of Subsurface Oxidation on the Structure, Stability, and Reactivity of Grafted Si(111) Surfaces. *J. Phys. Chem. C* **2008**, *112*, 14867−14877.
(24) Henkelman, G.; Uberuaga, B. P.; Jónsson, H. A Climbing Image Nudged Elastic Band Method for Minding Saddle Points and Minimum Energy Paths. *J. Chem. Phys.* **2000**, *113*, 9901−9905.
(25) Hurley, P. T.; Nemanick, E. J.; Brunschwig, B. S.; Lewis, N. S. Covalent Attachment of Acetylene and Methylacetylene Functionality to Si(111) Surfaces: Scaffolds for Organic Surface Functionalization while Retaining Si−C Passivation of Si(111) Surface Sites. *J. Am. Chem. Soc.* **2006**, *128*, 9990−9991.
(26) Rosso, M.; Giesbers, M.; Schroen, K.; Zuilhof, H. Controlled Oxidation, Biofunctionalization, and Patterning of Alkyl Monolayers on Silicon and Silicon Nitride Surfaces Using Plasma Treatment. *Langmuir* **2010**, *26*, 866−872.
(27) Aureau, D.; Morscheidt, W.; Etcheberry, A.; Vigneron, J.; Ozanam, F.; Allongue, P.; Chazalviel, J.-N. Controlled Oxidation of Alkyl Monolayers Grafted onto Flat Si(111) in an Oxygen Plasma of Low Power Density. *J. Phys. Chem. C* **2009**, *113*, 14418−14428.
(28) Zhang, F.; Liu, D.; Zhang, Y.; Wei, H.; Song, T.; Sun, B. Methyl/Allyl Monolayer on Silicon: Efficient Surface Passivation for Silicon-Conjugated Polymer Hybrid Solar Cell. *ACS Appl. Mater. Interfaces* **2013**, *5*, 4678−4684.

DOI: 10.1021/jp508728v
J. Phys. Chem. C XXXX, XXX, XXX−XXX